Semi analytical solution of MHD Non-aligned Stagnation-point flow of Nanofluid over a Stretching Surface in a Porous Medium with a Convective Boundary Condition

Asha S. K[*] and Gayitri Mali[1]

[*, 1]Department of Mathematics, Karnatak University, Dharwad, Karantaka, India

Email: as.kotnur2008@gmail.com

Abstract: The stagnation-point flow over a stretched surface is concerned in many industrial processes such as soft sheet extrusion, metal spinning, and paper production. On the account of these possible engineering applications, the study of stagnation-point flows has received a lot of attention. In the present paper, the non-aligned stagnation-point flow has found to be interesting and innovative in the analysis of viscous nanofluid over stretching surface with a convective boundary condition in presence of porous medium and magnetic effect. The suitable similarity transformation is utilized for the reduction of a set of governing equations, which are solved by using the differential transformation method (DTM) with the aid of MAPLE software. The effect of different physical parameters on flow is shown with the help of graphsThe skin friction, the Nusselt number, and Sherwood number are tabulated. Further, velocity, temperature, and nanoparticle volume fraction profiles are shown graphically and physical parameters are discussed. The comparison of the obtained results with a fourth-order Runge–Kutta–Fehlberg integration scheme with shooting technique is made.

Keywords: Non-aligned stagnation-point flow, stretching surface, porous medium, magnetic effect.

1. Introduction

In several industrial and engineering processes, prominent importance of flow over stretching sheet can be seen. For instance, in polymer sheets extrusion, production of glass-fiber and paper, wire drawing, metal-spinning. In such cases, the rate of cooling and stretching are very much needed in obtaining the desired final quality of the product. The theory of flow over a stretching plate was coined by **Crane L.J(1970).** Stagnation-point flows over stretched surfaces are common in industrial processes such as soft sheet extrusion, metal spinning, and paper production. Because of its usefulness in many engineering applications, the study of stagnation-point flows has received a lot of attention. A solid wall can stifle flow in some cases, whereas a free stagnation point or line can exist inside the fluid domain. A rigid or stretched wall covers the entire horizontal axisin a stagnation point, and the domain of fluid is > 0 . The fluid strikes the wall in an orthogonal or oblique manner. This simple model of an oblique stagnation point assists us to know how a boundary layer forms. As a result, the position of the stagnation point is essential for understanding boundary layer behaviour. The study of this oblique stagnation point flow has piqued researchers' interest due to its numerous engineering and industrial applications, including solar central receivers uncovered to wind current, cooling of nuclear reactors during an emergency shutdown (**Burde, 1995**). **Stuart (1959)** was first to study the oblique stagnation point flow of a fluid approaching a fixed rigid surface. Later, **Tamada (1979)** and **Dorrepaal (1986)** independently examined this problem. Further, Reza and Gupta (2005) investigated the flow of a fluid approaching a stretching surface from an oblique stagnation point. Some investigations on oblique stagnation-point flow are (**Mahapatra*et al.,* 2012; Nadeem*et al.,* 2013; Makinde*et al.,* 2016 ; JayachandraBabu*et al.,* 2016; Vijaya*et al.,* 2019**)..

Various examinations of the flow of water in porous media have been conducted during the last few decades. Fluid flow across a porous medium offers a wide range of physical and industrial applications. Fiber and granular insulation, building thermal insulation, food processing and storage, and underground heavy water disposal are just a few examples. Flow through a porous medium saturated with fluid is significant in a variety of technological applications, and it is becoming more important as the use of geothermal energy and astrophysical difficulties grows. In porous media, knowing of fundamentals of mass, energy, and momentum transport could benefit a variety of other applications, including nuclear reactor cooling, nuclear waste disposal underground, food processing, petroleum reservoir operations, building insulation, and welding in manufacturing processes. **Raptis and Takhar (1987)** were among the first to investigate the flow through a porous medium over a semi-infinite plate. Several attempts have been to investigate the porous medium in various circumstances **(Seddeek, 2007; Rehman*et al.,* 2013; Reddy *et al.,*2021; Megahedand Abbas, 2022 ; Gul*et al.,*2018; Ullah*et al.,* 2020).**

In current metallurgical and metal-working operations, the study of magneto-hydrodynamic (MHD) movement of an electrically conducting fluid is of great passion. The application of a magnetic field to fuse metals in an electrical furnace and the cooling of the wall within a nuclear reactor container are two examples of such fields **(Ibrahim *et al.,* 2013).** Hydro-magnetic techniques are used to purify molten metals from non-metallic impurities by applying a magnetic field to them. As a result, the problem we are working on is extremely

beneficial to polymer technology and metallurgy. A few other interesting works on magnetic effect are **(Ishaka*et al.*, 2009; Maboode*t al.*, 2017; Rajendar*et al.*, 2017; Uka and Amos, 2022)**

Nanofluid is said to be a composite of solid-liquid mixture of nanoparticles of sizes 1-100nm. It consists of a liquid called base fluid such as ethyl glycol, water, oil etc., and solid particles known as nanoparticles. The term nanofluid was first investigated by **Choi (1995).** The use of nanofluid is essential due to their high thermal conductivity properties. This study has applications in the areas of blowing and spinning of glass, paper production, drawing of wires and sheets of fiber, steel, metals and aluminum alloy spinning, and drawing of plastic films. During the processes, the transfer of heat between the sheet and medium of the fluid takes place and as a result of this, the material needs to be stretched. Meanwhile, the cooling and stretching of the sheet is very important, hence the quality of the product is dependent on the rate at which the cooling and stretching takes place. Some studies on nanofluids can be seen in **(Mehmood*et al.*, 2015; Khan and Pop, 2012; Rizwan and Nadeem, 2014; Das *et al.*, 2015; Makinde and Aziz, 2011)**

From the above mentioned literature, the problem of non-aligned stagnation point flow of nanofluid over stretching surface in a porous medium with a convective boundary condition the presence of magnetic effect with DTM is not yet studied. The set of ordinary differential equations which are obtained by using appropriate similarity transformation are highly nonlinear, and are solved by using semi-analytical method known as differential transformation method (DTM) **(Sepasgozar*et al.*,2017;Ganji and Mirzaaghaian, 2016;Hatami and Jing, 2016).**

2.Significance Of The Study

The stagnation-point flow over stretched surface is concerned in many industrial processes such as soft sheet extrusion, metal spinning, and paper production. On the account of these possible engineering applications, the study of stagnation-point flows has received a lot of attention. In the present paper, the non-aligned stagnation-point flow has found to be interesting and innovative in the analysis of viscous nanofluid over stretching surface with a convective boundary condition in presence of porous medium and magnetic effect.

3. Methodology:

The suitable similarity transformation is utilized for the reduction of a set of governing equations, which are solved by using the differential transformation method (DTM). The skin friction, the Nusselt number, and Sherwood number are tabulated. Further, velocity, temperature, and nanoparticle volume fraction profiles are shown graphically and studied in detail for various physical parameters. The comparison of the obtained results with a fourth-order Runge–Kutta–Fehlberg integration scheme with shooting technique is made and an excellent agreement is found.

4. Findings:

It is noticed that as the magnetic parameter enhances, the temperatureand nanoparticle volume fraction profiles reduces but the opposite behaviour can be seen in the velocity profile. Enhancement in the effect of the porosity parameter diminishes the velocity profile while enhance the temperature profile.

5. Originality:

To the best of the author's knowledge, so far the problem of non-aligned stagnation point flow of nanofluid over stretching surface in a porous medium with a convective boundary condition in presence of magnetic effect by differential transform method is not yet studied.

6. Mathematical Formulation

By maintaining the origin stationary with the velocity $\hat{\hat{U}}_W(x) = cx$, the sheet is stretched along the x-axis by two equal and opposite forces. Outside the boundary layer, let $\hat{\hat{U}}_\infty(x) = ax + by$ be the fluid velocity as shown in figure. 1.

The governing equations are given below

$$\frac{\partial \hat{\hat{u}}}{\partial x} + \frac{\partial \hat{\hat{v}}}{\partial y} = 0, \tag{1}$$

$$\hat{\hat{u}}\frac{\partial \hat{\hat{u}}}{\partial x} + \hat{\hat{v}}\frac{\partial \hat{\hat{u}}}{\partial y} = \hat{\hat{U}}_\infty \frac{\partial \hat{\hat{U}}_\infty}{\partial x} + \nu_f \frac{\partial^2 \hat{\hat{u}}}{\partial y^2} + g\beta(\hat{\hat{T}} - \hat{\hat{T}}_\infty) + g\beta^*(\hat{\hat{C}} - \hat{\hat{C}}_\infty) - \left(\frac{\sigma {B_0}^2}{\rho_f} + \frac{\nu_f}{K}\right)\left(\hat{\hat{u}} - \hat{\hat{U}}_\infty\right), \tag{2}$$

$$\hat{\hat{u}}\frac{\partial \hat{\hat{T}}}{\partial x} + \hat{\hat{v}}\frac{\partial \hat{\hat{T}}}{\partial y} = \alpha_f \frac{\partial^2 \hat{\hat{T}}}{\partial y^2} + \tau\left\{D_B\left(\frac{\partial \hat{\hat{C}}}{\partial y}\frac{\partial \hat{\hat{T}}}{\partial y}\right) + \frac{D_T}{T_\infty}\left(\frac{\partial \hat{\hat{T}}}{\partial y}\right)^2\right\}, \tag{3}$$

$$\hat{u}\frac{\partial \hat{\hat{C}}}{\partial x}+\hat{v}\frac{\partial \hat{\hat{C}}}{\partial y}=D_B\frac{\partial^2 \hat{\hat{C}}}{\partial y^2}+\frac{D_T}{T_\infty}\frac{\partial^2 \hat{\hat{T}}}{\partial y^2}. \tag{4}$$

The boundary conditions are as follows

$$\hat{u}=\hat{\hat{U}}_W=cx,\ \hat{v}=0,\ -k\frac{\partial \hat{\hat{T}}}{\partial y}=h_f\left(\hat{\hat{T}}_f-\hat{\hat{T}}\right),\ \hat{\hat{C}}=\hat{\hat{C}}_W \text{ at } y=0, \tag{5}$$

$$\hat{u}=\hat{\hat{U}}_\infty=ax+by,\ \hat{\hat{T}}\to\hat{\hat{T}}_\infty,\ \hat{\hat{C}}\to\hat{\hat{C}}_\infty \text{ as } y\to\infty. \tag{6}$$

Non-dimensional similarity variables as follows:

$$\eta=y\sqrt{\frac{c}{\nu_f}},\ X=x\sqrt{\frac{c}{\nu_f}},\ \hat{u}=\sqrt{c\nu_f}\left[Xf'+g'\right],\ \hat{v}=-\sqrt{c\nu_f}\,f(\eta),$$

$$\psi=\nu_f\left[Xf(\eta)+g(\eta)\right],\ \theta(\eta)=\frac{\hat{\hat{T}}-\hat{\hat{T}}_\infty}{\hat{\hat{T}}_f-\hat{\hat{T}}_\infty},\ \phi(\eta)=\frac{\hat{\hat{C}}-\hat{\hat{C}}_\infty}{\hat{\hat{C}}_W-\hat{\hat{C}}_\infty}. \tag{7}$$

$\psi=\nu_f\left[Xf(\eta)+g(\eta)\right]$, is :

$$\hat{u}=\sqrt{\frac{c}{\nu_f}}\frac{\partial\psi}{\partial\eta},\ \hat{v}=-\sqrt{\frac{c}{\nu_f}}\frac{\partial\psi}{\partial X}. \tag{8}$$

Here, $f(\eta)$ and $g(\eta)$ are the normal and tangential components of flow.

Eq. (1) is automatically satisfied by using (8) and Eqs. (2) - (4) are reduced into ordinary differential equations as given below:

$$f'''+ff''-\left(f'\right)^2+\left(M+K_p\right)\left(\lambda_1-f'\right)+\lambda_1^2+Grt\theta+Grc\phi=0, \tag{9}$$

$$g''+fg'-f'g'+\left(M+K_p\right)\left(\lambda_2\eta-g'\right)+\lambda_2 S=0, \tag{10}$$

$$\theta''+\Pr\left\{f\theta'+Nb\phi'\theta'+Nt\left(\theta'\right)^2\right\}=0, \tag{11}$$

$$\phi''+\Pr Lef\phi'+\frac{Nt}{Nb}\theta''=0. \tag{12}$$

Boundary conditions (5) and (6) are transformed as follows,

$$f=0,\ f'=1,\ g'=0,\ \theta'=-Bi\left[1-\theta(\eta)\right],\ \phi=1 \text{ at } \eta=0, \tag{13}$$

$$f'=\lambda_1,\ g''=\lambda_2,\ \theta\to0,\ \phi\to0 \text{ as } \eta\to\infty. \tag{14}$$

From Eq. (14), it can be easily seen that $f(\eta)=\lambda_1\eta+S$ as $\eta\to\infty$.

Let $g^1=\lambda_2 G(\eta).$ (15)

Substituting Eq. (15) into Eq. (10), (13) and (14), we obtain

$$G''(\eta)+fG'(\eta)-f'G(\eta)+\left(M+K_p\right)\left(\eta-G(\eta)\right)+S=0, \tag{16}$$

$$f=0,\ f'=1,\ G=0,\ \theta'=-Bi\left[1-\theta(\eta)\right],\ \phi=1 \text{ at } \eta=0, \tag{17}$$

$$f'=\lambda_1,\ G'=1,\ \theta\to0,\ \phi\to0 \text{ as } \eta\to\infty. \tag{18}$$

The parameters are defined as:

$$\lambda_1=\frac{a}{c},\ \lambda_2=\frac{b}{c},\ Nt=\frac{\tau D_T\left(\hat{\hat{T}}_f-\hat{\hat{T}}_\infty\right)}{\nu_f\hat{\hat{T}}_\infty},\ Nb=\frac{\tau D_B\left(\hat{\hat{C}}_W-\hat{\hat{C}}_\infty\right)}{\nu_f},\ \Pr=\frac{\nu_f}{\alpha_f},\ \nu_f=\frac{\mu_f}{\rho_f},\ Le=\frac{\alpha_f}{D_B}, \tag{19}$$

$$M=\frac{\sigma B_0^{\ 2}}{\rho_f c},\ Bi=\frac{h_f}{k}\sqrt{\frac{\nu_f}{c}},\ \alpha_f=\frac{k}{\left(\rho c_p\right)_f},\ K_p=\frac{\nu_f}{cK},\ Grt=\frac{g\beta\left(\hat{\hat{T}}_f-\hat{\hat{T}}_\infty\right)}{c^2x},$$

where C_f, Nu_x and Sh_x are given below:

$$C_f=\frac{\tau_W}{\rho_f U_W^{\ 2}},\ Nu_x=\frac{xq_W}{k(\hat{\hat{T}}_f-\hat{\hat{T}}_\infty)},\ Sh_x=\frac{xq_m}{k(\hat{\hat{C}}_W-\hat{\hat{C}}_\infty)}. \tag{20}$$

$$\tau_W = \mu_f \left(\frac{\partial \hat{u}}{\partial y}\right)_{y=0}, \; q_W = -k\left(\frac{\partial \hat{T}}{\partial y}\right)_{y=0} \quad q_m = -D_B\left(\frac{\partial \hat{C}}{\partial y}\right)_{y=0}. \quad (21)$$

Using Eq. (23) in Eq. (22), we obtain

$$C_f = \left(Xf''(0) + g''(0)\right), \; Nu = -\theta'(0) \text{ and } Sh = -\phi'(0). \quad (22)$$

7. Method of solution:

The reduced governing equations (9), (11), (12) and (16) with the boundary conditions (17) and (18) are resolved by utilizing DTM method and we get the following equations (23) - (26).

$$(i+1)(i+2)(i+3)F[k+3] + \sum_{r=0}^{i}(i+1)F[i-r](i+2)F[i+2]$$
$$-\sum_{r=0}^{i}(i+1)(i-r+1)F[i-r+1]F[i+1] - (i+1)(M+K_p)F[i+1] + \left[(M+K_p)\lambda_1 + \lambda_1^2\right]\delta(i) + GrtT[i] + GrcP[i] = 0, \quad (23)$$

$$(i+1)(i+2)T[i+2] + \Pr\left\{\sum_{r=0}^{i}(r+1)F[i-r]T[r+1] + Nb\sum_{r=0}^{i}(r+1)T[i-r+1](i-r+1)P[r+1]\right\} +$$
$$\Pr\left\{Nt\sum_{r=0}^{i}(i+1)T[i-r+1](i-r+1)T[i+1]\right\} = 0, \quad (24)$$

$$(i+1)(i+2)P[i+2] + \Pr Le\left\{\sum_{r=0}^{i}(r+1)F[i-r]P[r+1]\right\} + (i+1)\frac{Nt}{Nb}(i+2)T[i+2] = 0, \quad (25)$$

$$(i+1)(i+2)H[i+2] - \sum_{r=0}^{i}(r+1)H[i-r]F[r+1] + \sum_{r=0}^{i}(r+1)F[i-r]H[r+1] - (M+K_p)H[i] + (M+K_p)\delta(i-1) + S\delta(i) = 0. \quad (26)$$

Transformed boundary conditions are:

$$F[0] = 0, \; F[1] = 1, \; F[2] = \frac{b}{2}, \; H[0] = 0, \; H[1] = e, \; T[0] = \frac{Bi - c}{Bi},$$
$$T[1] = c, \; P[0] = 1, \; P[1] = d. \quad (27)$$

Differential transform of $f(\eta), \theta(\eta), \phi(\eta), G(\eta)$ are $F(i), T(i), P(i), H(i)$ and with the help of boundary conditions (17)-(18), we can find constants b, c, d *and* e. By utilizing transformed boundary conditions (27) and equations (23)-(26), we obtain the closed form of solution.

8. Result and discussion

The results are shown in Figure 2–16 and explored in detail to demonstrate the characteristics of the problem. Sh, Nu, and C_f are all tabulated. With a fourth-order Runge–Kutta–Fehlberg integration scheme and shooting technique, the accuracy of the acquired results is checked, and an excellent agreement is found which are shown in table 1 and table 2.

Table 1: Coefficient of $f''(0)$ with $M = 0, \; K_p = 0, \; \beta = 0$.

	Present results			Results obtained by Makinde*et al.*2016		
λ_1	S	$f''(0)$	$G'(0)$	S	$f''(0)$	$G'(0)$
0.1	0.791705	-0.969386	0.26332	-0.791705	-0.969386	0.26332
0.2	-	-0.919209	-	-	-	-
0.3	0.519499	-0.849420	0.60631	-0.519499	- 0.849420	0.60631
0.8	-	-	-	-0.114527	-0.299388	0.93472
2	0.410407	2.017502	1.16521	0.410407	2.017502	1.16521
3	0.693053	4.729282	-	0.693053	4.729282	1.23465

Table 2: Comparison with Makinde*et al.*2016 when $\lambda_1 = \beta = Nr = M = K_p = 0,\ \Pr = 10,\ Le = 10,\ Bi = 0.1.$

	Present results				Results obtained by Makinde*et al.*2016			
Nt	$-\theta'(0)$ $Nb = 0.1$	$-\phi'(0)$ $Nb = 0.1$	$-\theta'(0)$ $Nb = 0.5$	$-\phi'(0)$ $Nb = 0.5$	$-\theta'(0)$ $Nb = 0.1$	$-\phi'(0)$ $Nb = 0.1$	$-\theta'(0)$ $Nb = 0.5$	$-\phi'(0)$ $Nb = 0.5$
0.1	0.092135	2.277412	0.038331	2.356031	0.0921	2.27741	0.03833	2.35603
0.2	0.092551	2.222812	0.026901	2.457621	0.09255	2.22281	0.02690	2.45762
0.3	0.092121	2.178343	0.018001	2.543524	0.09212	2.17834	0.01800	2.54352

8.1 Velocity Profile

The impact of the magnetic parameter M on the axial and oblique velocity gradient profiles (i.e. $f'(\eta)$ and $G'(\eta)$)in the boundary layer is seen in figures 2 and 7. The Lorentz force is a resistive-type force that occurs when a transverse magnetic field is applied to an electrically conducting fluid and has a propensity to slow down the fluid in the boundary layer. As a result, the axial velocity drops. Figures 3 and 8 shows that the axial velocity as well as oblique velocity gradient profiles diminishes as values of porosity parameter K_p increases. Because, increasing K_p amplifies the porous layer and thereby reduces the thickness of momentum boundary layer. In figures 4 and 5, as the values of thermal Grashof number Grt and the solutalGrashof number Grc rise, $f'(\eta)$ and $G'(\eta)$ also rise. The ratio of the buoyant force to the viscous force is known as Grt in this context. It is noted that the flow is accelerated as a result of the buoyant force being increased in accordance with the rising thermal Grt for fluids. The buoyant force to viscous hydrodynamic force ratio is known as Grc. Thus, as hydrodynamic force increases and buoyancy force remains constant, the thickness of the momentum boundary layer decreases. The effect of the velocity ratio parameter λ_1 on $f'(\eta)$ and $G'(\eta)$ is depicted in figure 6 and 9. When $U_e(x)$ exceeds $U_w(x)$, the flow velocity increases, and the thickness of the boundary layer reduces as λ_1 rises. Furthermore, when $U_e(x) < U_w(x)$, the flow field velocity reduces, as does the thickness of the boundary layer. The flow exhibits an inverted boundary layer structure when $\lambda_1 < 1$.

8.2 Temperature Profile and nanoparticles volume fraction

The effect of M on $\theta(\eta)$ in the boundary layer is demonstrated in figure 10. The Lorentz force is a resistive-type force that is produced when a transverse magnetic field is applied to an electrically conducting fluid. This force tends to delay the fluid's velocity and raise its temperature in the boundary layer. In addition, when the magnetic field intensity increases, the impacts on flow and heat fields become more prominent. As shown in figure 11, temperature profiles rise when the porosity parameter K_p rises. Due to the expansion of the fluid's pores, K_p develops a resistance force that opposes the flow field and raises the thickens the thermal boundary layer.The effect of Biot number Bi on the thermal boundary layer is depicted in figure. 12. Higher surface temperatures are caused by stronger convection, which increases the thermal effect to penetrate deeper into the static fluid, as predicted. With an increase in λ_1, the dimensionless $\theta(\eta)$ drops, diminishing the thickness of the thermal boundary layer and therefore the thermal resistance as shown in figure 13. Figure 14 shows that as Lewis number Le rises nanoparticle volume fraction profile $\phi(\eta)$) degrades, Le and Brownian diffusion coefficient are of opposite behaviour as Le rises Brownian diffusion coefficient reduces. Figure 15 illustrates that $\phi(\eta)$ increases as the values of Nt increases. The influence of the M on $\phi(\eta)$ in the boundary layer is seen in figure 15. The Lorentz force is a resistive-type force and has the effect of slowing the velocity of the fluid in the boundary layer and creating a higher concentration of nanoparticles in the fluid.

8.3 Streamlines

Figures 16 (a) to 16 (c) shows the streamlines patterns for oblique flow. The streamlines are inclined left for positive values of λ_2 as shown in figure 16 (a) and right for negative values of λ_2 in figure 16 (c), as expected. When $\lambda_2 = 0$, the streamlines are found to be normal to the surface in figure 16(b). This is because raising the velocity ratio parameter λ_2 enhances shearing motion, which causes the flow to become increasingly obliquity towards the stretched surface.

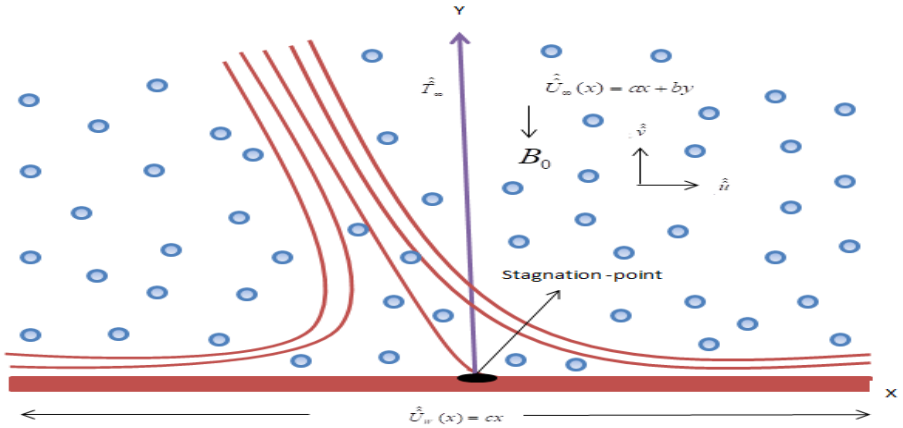

Figure 1 Physical model

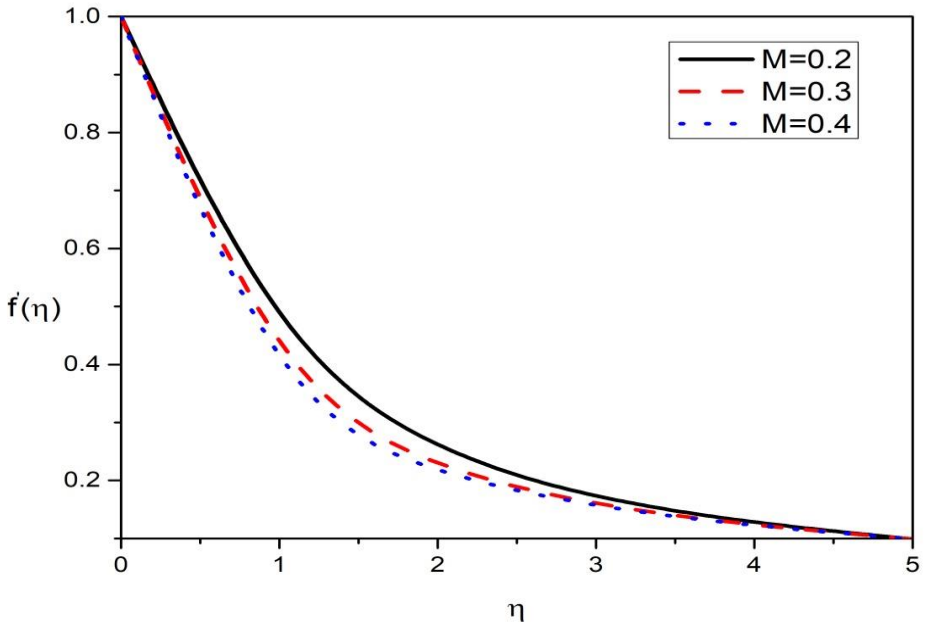

Figure 2: Variation of $f'(\eta)$ on M

$\lambda_1 = 0.1, Bi = 0.1, Nb = 0.5, Grt = 0.2, Nt = 0.5, K_p = 0.5, Grc = 0.2, Le = 5, \Pr = 2.$

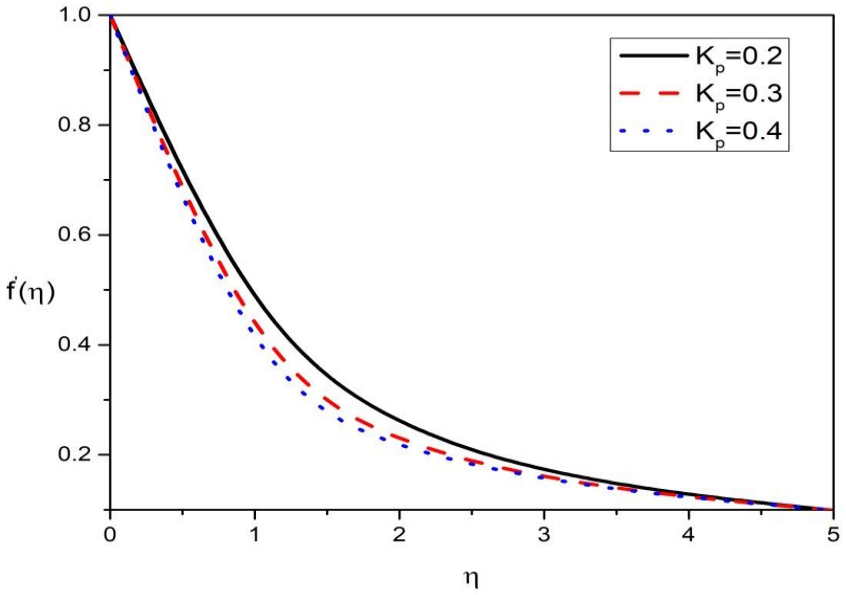

Figure 3: Variation of $f'(\eta)$ on K_p

$\lambda_1 = 0.1, Bi = 0.1, Nb = 0.5, Grt = 0.2, M = 0.3, Nt = 0.5, Grc = 0.2, Le = 5, \Pr = 2.$

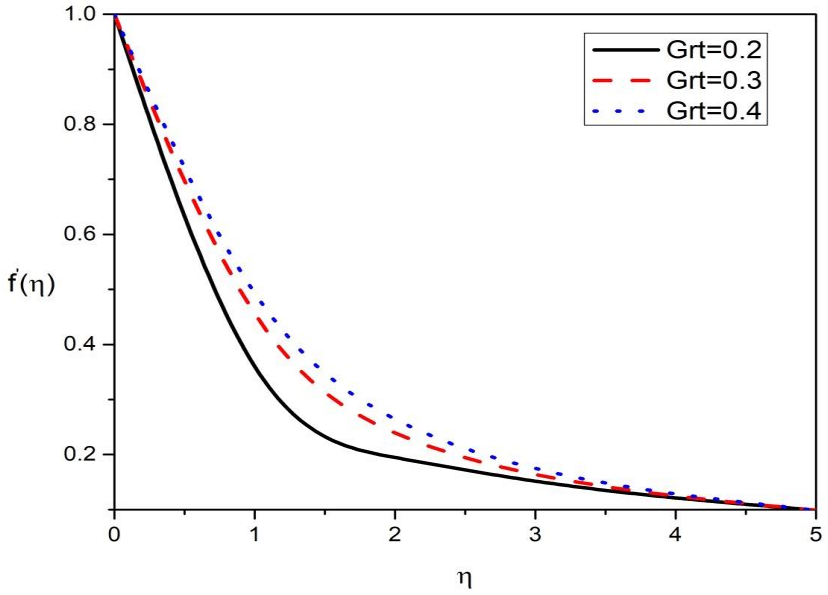

Figure 4: Variation of $f'(\eta)$ on Grt

$\lambda_1 = 0.1, Bi = 0.1, Nb = 0.5, K_p = 0.3, M = 0.3, Nt = 0.5, Grc = 0.2, Le = 5, \Pr = 2.$

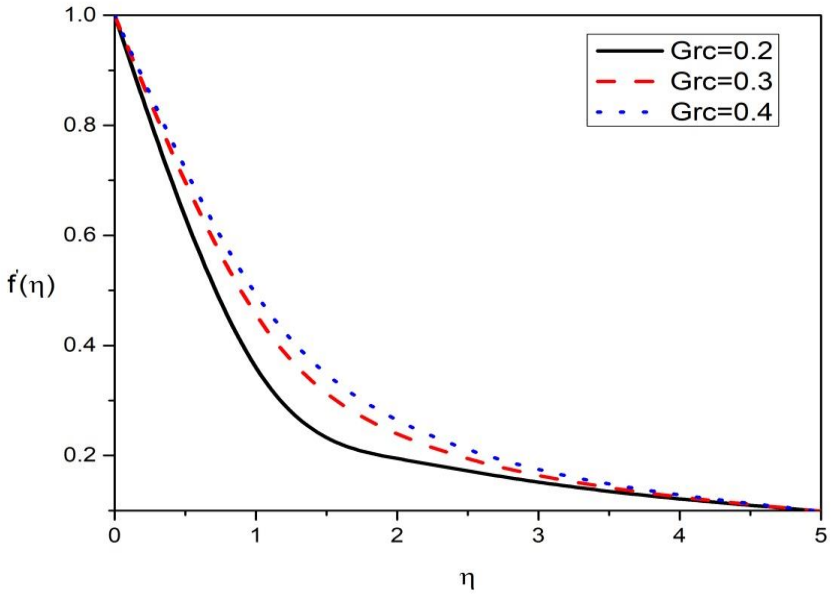

Figure 5: Variation of $f'(\eta)$ on Grc

$\lambda_1 = 0.1, Bi = 0.1, Nb = 0.5, K_p = 0.3, M = 0.3, Nt = 0.5, Grt = 0.2, Le = 5, \Pr = 2.$

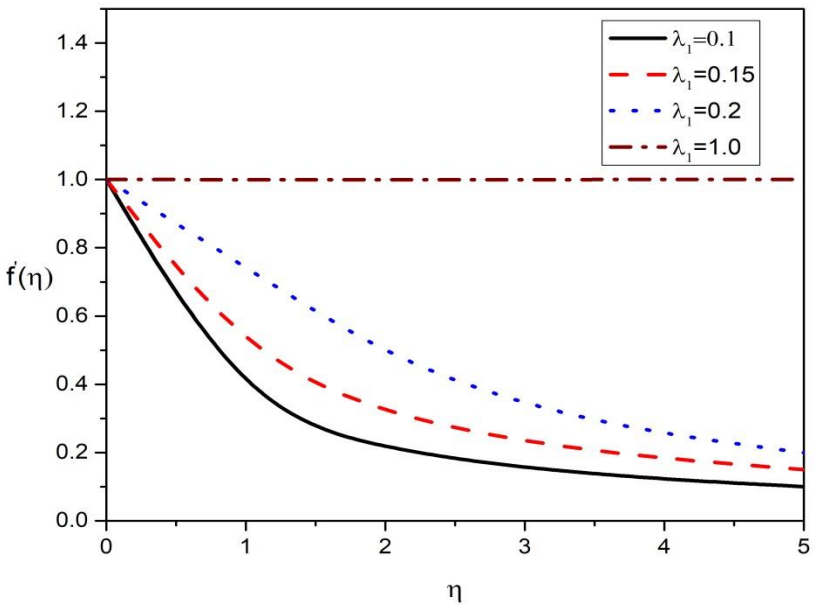

Figure 6: Variation of $f'(\eta)$ on λ_1

$Grc = 0.2, Bi = 0.1, Nb = 0.5, K_p = 0.3, M = 0.3, Nt = 0.5, Grt = 0.2, Le = 5, \Pr = 2.$

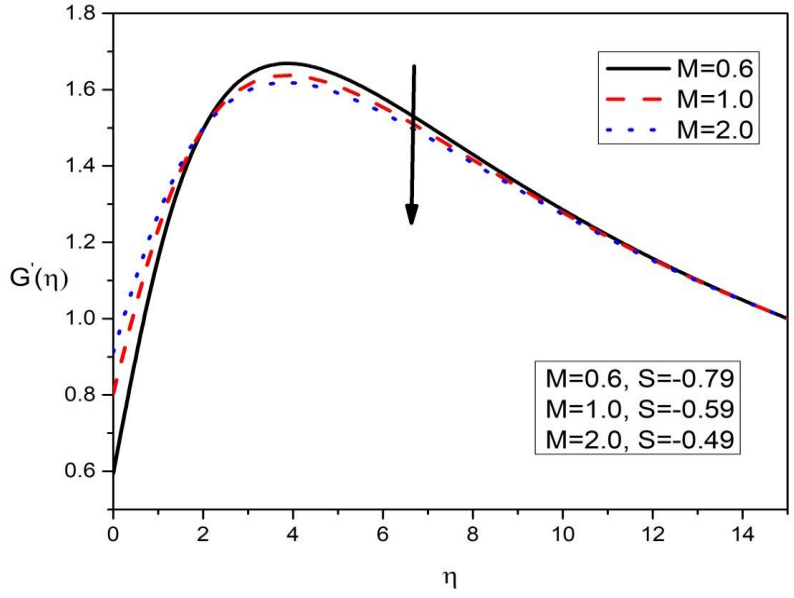

Figure 7: Variation of $G^{'}(\eta)$ on M

$Grc = 0.5, Bi = 0.1, Nb = 0.5, K_p = 0.3, Nt = 0.5, Grt = 0.5, Le = 100, \Pr = 2, \lambda_1 = 0.1,$

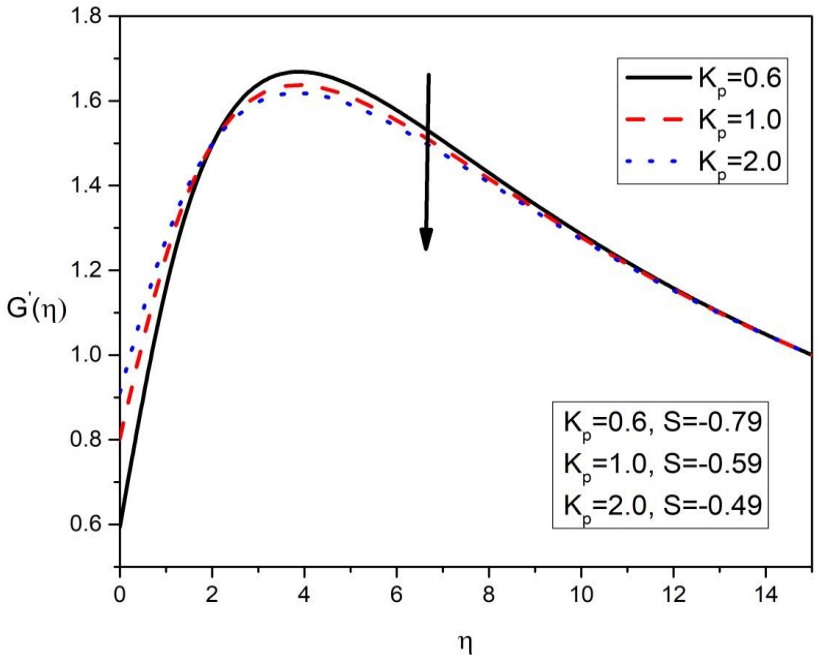

Figure 8: Variation of $G^{'}(\eta)$ on K_p

$Grc = 0.5, Bi = 0.1, Nb = 0.5, M = 0.3, Nt = 0.5, Grt = 0.5, Le = 100, \Pr = 2, \lambda_1 = 0.1,$

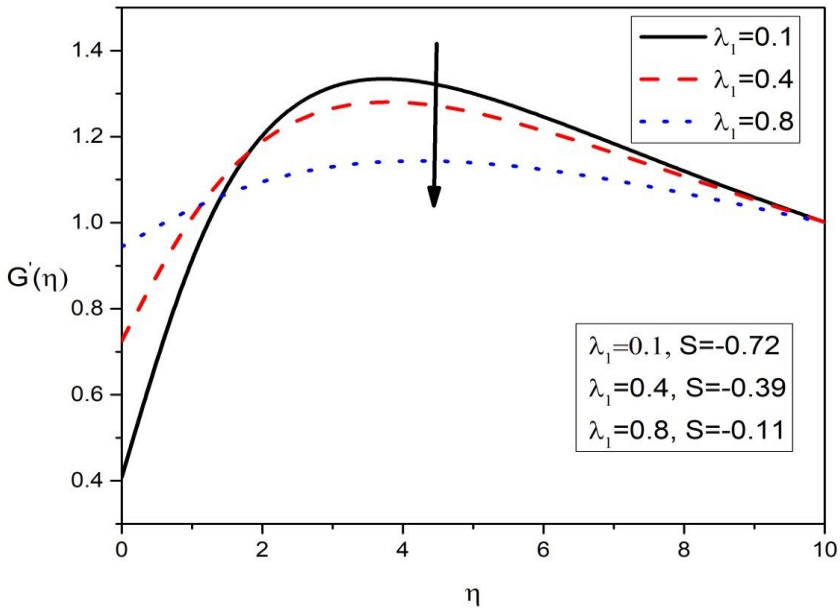

Figure 9: Variation of $G^{'}(\eta)$ on λ_1

$Grc = 0.5, Bi = 0.1, Nb = 0.5, M = 0.3, Nt = 0.5, Grt = 0.5, Le = 100, \Pr = 2, K_p = 0.3.$

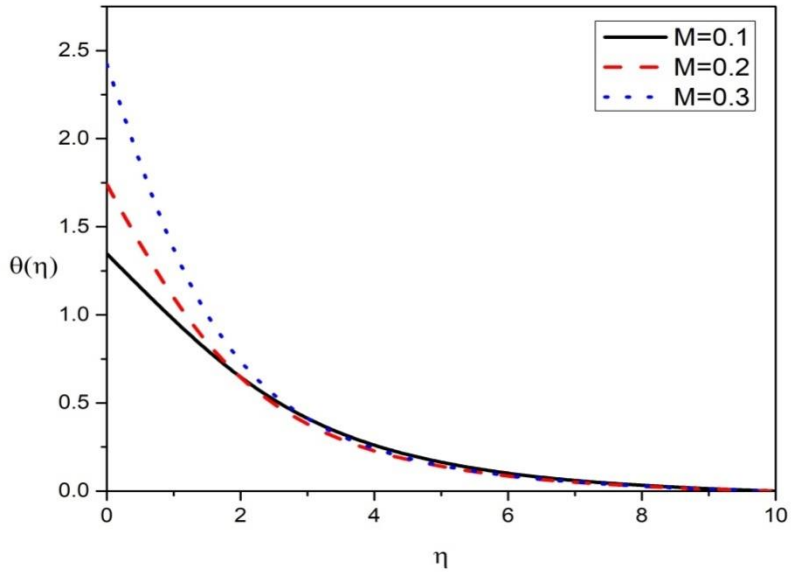

Figure 10: Variation of $\theta(\eta)$ on M

$Grc = 0.1, Nt = 0.1, Grt = 0.1, Le = 100, \Pr = 1, K_p = 0.3, \lambda_1 = 0.1, Nb = 0.1.$

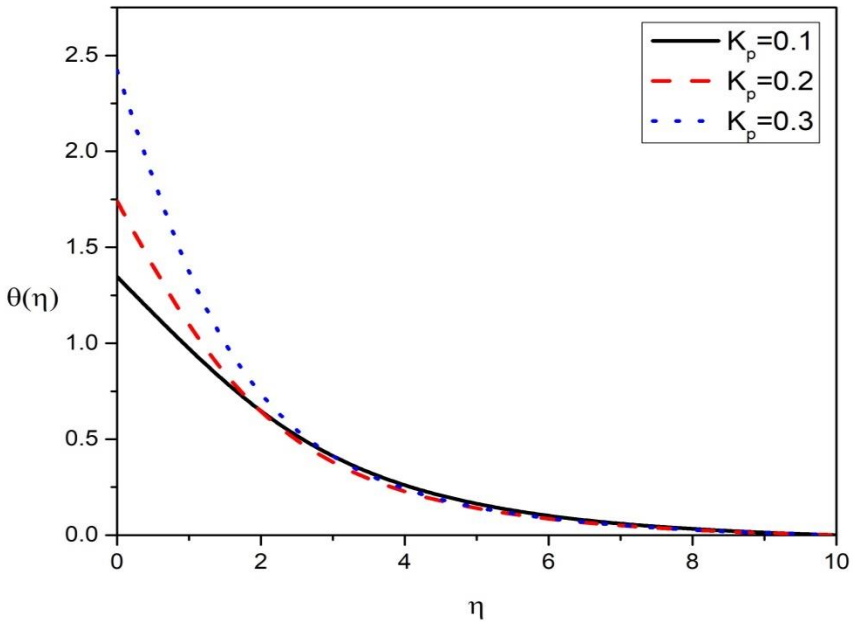

Figure 11: Variation of $\theta(\eta)$ on K_p

$Grc = 0.1, Nt = 0.1, Grt = 0.1, Le = 100, \Pr = 1, M = 0.3, \lambda_1 = 0.1, Nb = 0.1.$

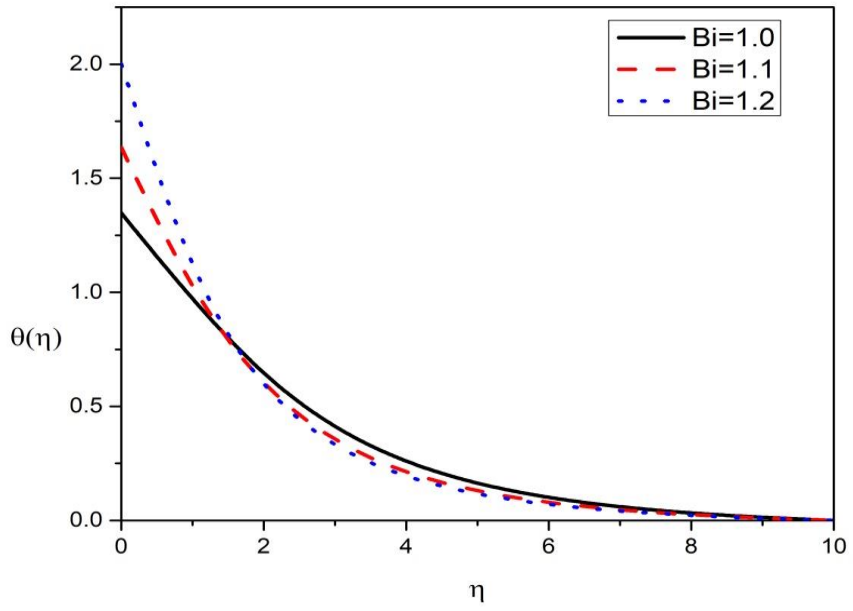

Figure 12: Variation of $\theta(\eta)$ on Bi

$Grc = 0.1, Nb = 0.1, M = 0.3, Nt = 0.1, Grt = 0.1, Le = 100, \Pr = 1, K_p = 0.3, \lambda_1 = 0.1.$

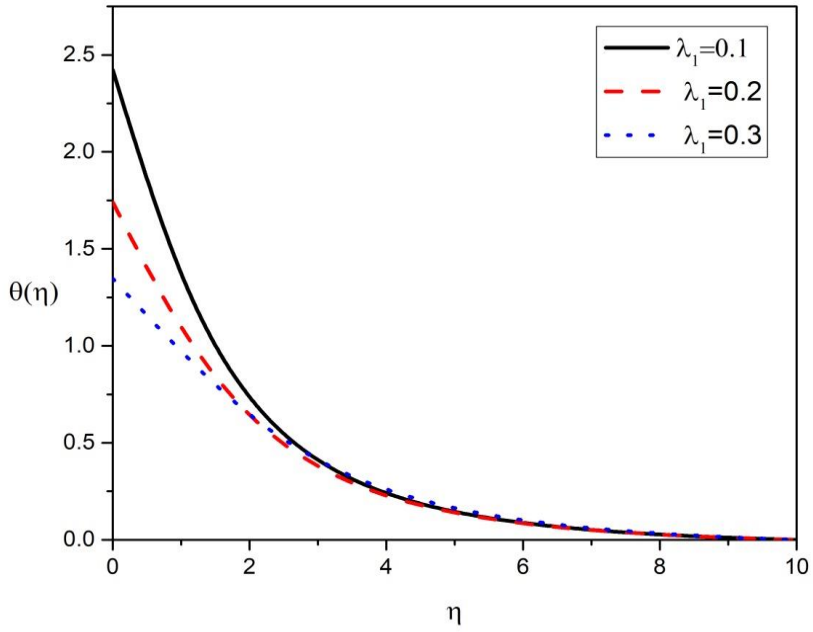

Figure 13: Variation of $\theta(\eta)$ on λ_1

$Grc = 0.1, Bi = 1, M = 0.3, Nb = 0.1, Grt = 0.1, Le = 100, Nt = 0.1, K_p = 0.3, \Pr = 1.$

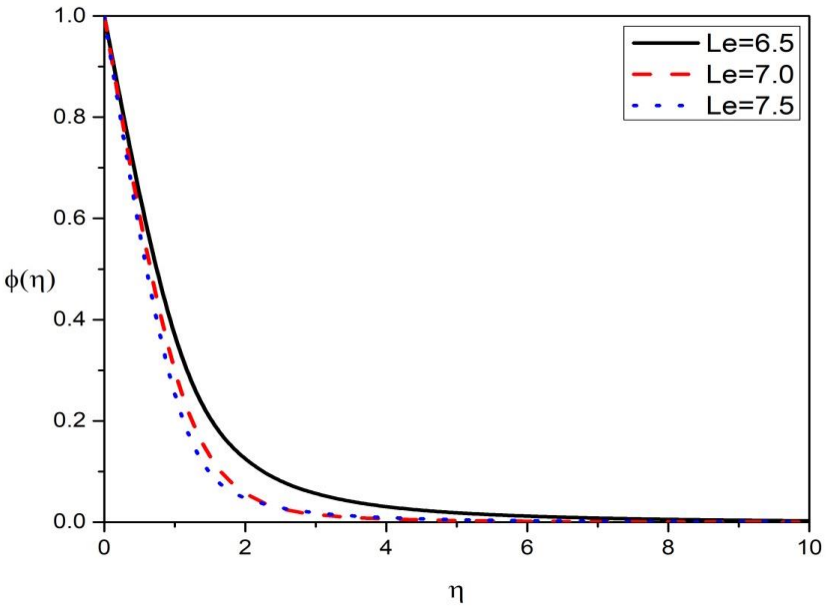

Figure 14: Variation of $\phi(\eta)$ on Le

$Grc = 0.1, Bi = 0.1, M = 0.3, Nb = 0.1, Grt = 0.1, Nt = 0.1, K_p = 0.3, \Pr = 1.$

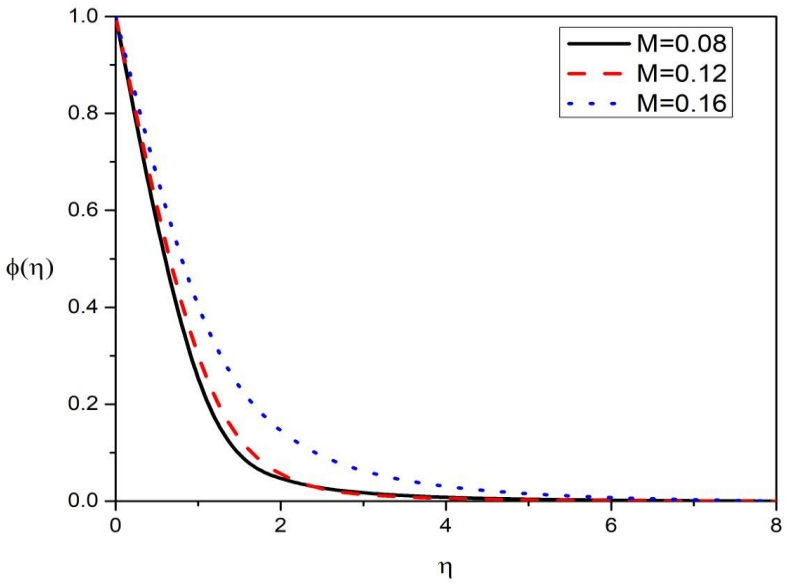

Figure 15: Variation of $\phi(\eta)$ on M

$Grc = 0.1, Bi = 0.1, Nt = 0.1, Nb = 0.1, Grt = 0.1, \lambda_1 = 0.1, K_p = 0.3, \Pr = 1.$

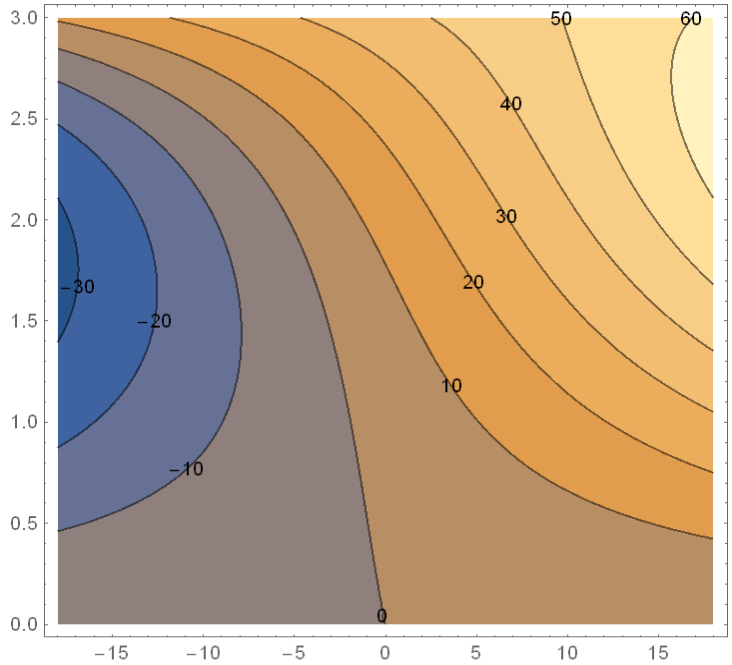

Figure 16 (a): Streamline patterns for the oblique flow for

$Grc = 0.1, Bi = 0.1, Grt = 0.1, K_p = 0.5, \Pr = 6, M = 0.5, \lambda_1 = 0.1, \lambda_2 = 2.5.$

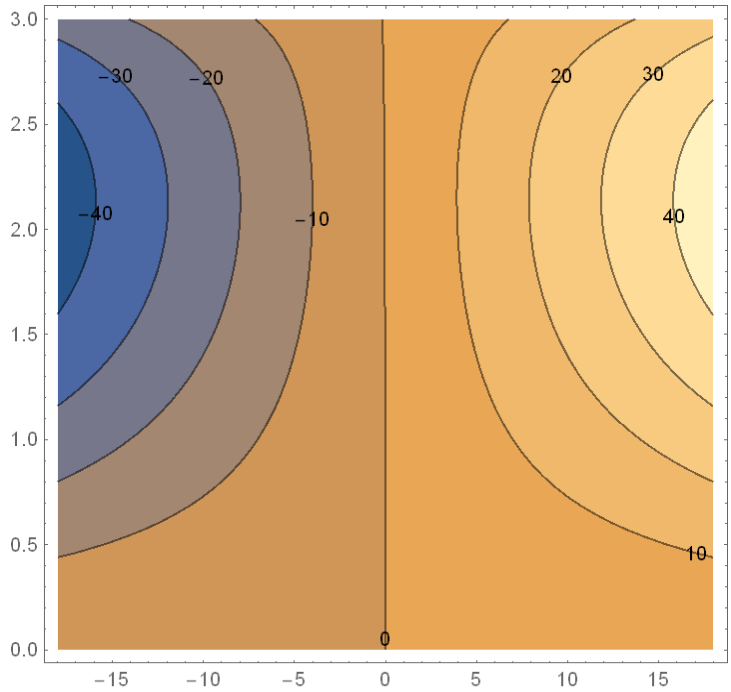

Figure 16(b): Streamline patterns for the oblique flow for

$Grc = 0.1, Bi = 0.1, Grt = 0.1, K_p = 0.5, \Pr = 6, M = 0.5, \lambda_1 = 0.1, \lambda_2 = 0$

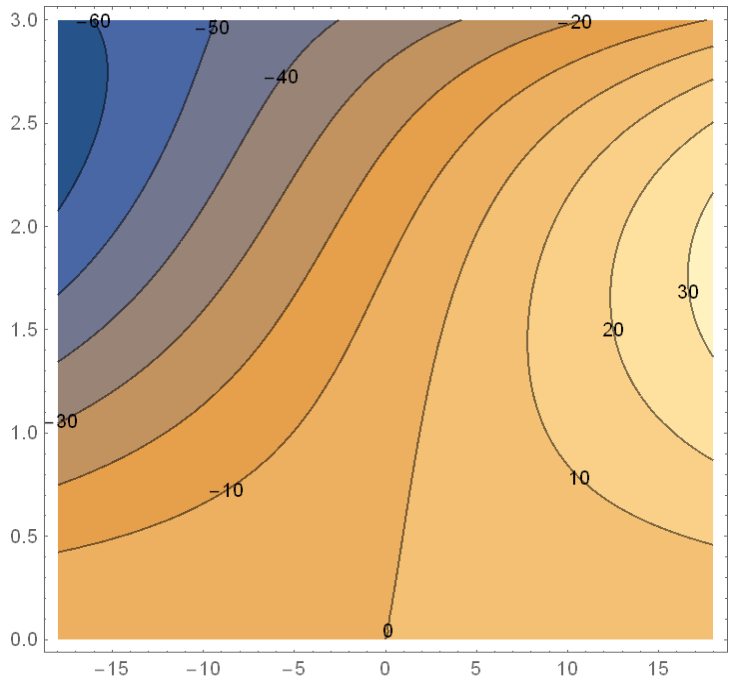

Figure 16(c): Streamline patterns for the oblique flow for
$Grc = 0.1, Bi = 0.1, Grt = 0.1, K_p = 0.5, \Pr = 6, M = 0.5, \lambda_1 = 0.1, \lambda_2 = -2.5.$

9. Conclusions:

Non-aligned Stagnation-point flow of Nanofluid over Stretching Surface in a Porous Medium with a Convective Boundary Condition in the presence of magnetic effect has been studied by using DTM. The outcome of various parameters is given below:

- As values of M increases, the axial velocity and oblique velocity gradient profiles decreases but opposite behavior can be seen in both $\theta(\eta)$ and $\phi(\eta)$.

- As values of K_p increases, temperature profile increases but opposite behavior can be seen in the axial velocity and oblique velocity gradient profiles.
- As values of λ_1 increases, similar behavior can be seen in both oblique velocity gradient and temperature profiles.
- As values of *Grt* and *Grc* rises, axial velocity profile increases.
- Increase in Biot number *Bi* increases the temperature profile..
- As *Le* rises, the nanoparticle volume fraction profile reduces.
- Streamline patterns for the oblique flow for different values of λ_2 can be seen.

References

Burde, G.I. 1995, "Non-steady Stagnation-Point Flows over Permeable Surfaces: Explicit Solutions of the Navier-Stokes Equations", *Journal of Fluids Engineering*, Vol.117 No. (1):189-191, doi: https://doi.org/10.1115/1.2816811.

Choi S.U.S. 1995, "Enhancing thermal conductivity of fluids with nanoparticle", in Stephen U.S., Eastman J.A. (Ed.s),*ASME international mechanical engineering congress and exposition*, San Francisco, CA, 12–17.

Crane, L.J. 1970, "Flow past a stretching plate", *Journal of Applied Mathematics and Physics*, 21(4):645–647, doi:https://doi.org/10.1007/BF01587695.

Das, S.,Chakraborty, S., Jana, R. N. and Makinde, O. D. 2015, "Entropy analysis of unsteady magneto-nanofluid flow past accelerating stretching sheet with convective boundary condition", *Applied Mathematics and Mechanics*, 36(12):1593–1610, doi:https://doi.org/10.1007/s10483-015-2003-6.

Dorrepaal, J.M. 1986, "An exact solution of the NavierStokes equation which describes Non-orthogonal stagnation-point flow in two-dimensions", *Journal of Fluid Mechanics*, 163:141–147, doi:https://doi.org/10.1017/S0022112086002240.

Ganji, D. D. and Mirzaaghaian, A. 2016,"Application of differential transformation method in micropolar fluid flow and heat transfer through permeable walls", *Alexandria Engineering Journal*, 55: 2183-2191,

doi:https://doi.org/10.1016/j.aej.2016.06.011.

Gul, T., Khan, N. S., Islam, S., Khan, I., Khan, W. and Ali, L. 2018, "Thin film flow of a second grade fluid in a porous medium past a stretching sheet with heat transfer", *Alexandria Engineering Journal*, 57 (2):1019–1031,
doi: https://doi.org/10.1016/j.aej.2017.01.036.

Hatami, M. and Jing, D. 2016, "Differential transformation method for Newtonian and non-Newtonian nanofluids flow analysis: compared to numerical solution", *Alexandria Engineering Journal*,55 :731-739, doi:https://doi.org/10.1016/j.aej.2016.01.003.

Ibrahim, W., Shankar, B. and Nandeppanavar, M. M. 2013, "MHD stagnation point flow and heat transfer due to nanofluid towards a stretching sheet", *International Journal of Heat and Mass Transfer*, 56 (1):1–9,
doi: 10.1016/j.ijheatmasstransfer.2012.08.034.

Ishaka, A., Jafar, K., Nazar, R. and Pop, I. 2009, "MHD stagnation point flow towards a stretching sheet", *Physica A*, 388(17):3377–3383,
doi: https://doi.org/10.1016/j.physa.2009.05.026.

JayachandraBabu, M. and Sandeep, N. 2016, "Effect of nonlinear thermal radiation on non-aligned bio-convective stagnation point flow of a magnetic-nanofluid over a stretching sheet", *Alexandria Engineering Journal*, 55(3):1931–1939,
doi: https://doi.org/10.1016/j.aej.2016.08.001.

Khan, W. A. and Pop, I. M. 2012, "Boundary Layer Flow Past a Stretching Surface in a Porous Medium Saturated by a Nanofluid: Brinkman-Forchheimer Model", *PLoSONE*, 7(10): e47031, doi: 10.1371/journal.pone.0047031.

Mabood, F.,Khan, W.A. and Ismail, A. I. Md. 2017, "MHD flow over exponential radiating stretching sheet using homotopy analysis method", *Journal of King Saud University – Engineering Sciences*, 29(1):68–74,
doi: https://doi.org/10.1016/j.jksues.2014.06.001.

Mahapatra, T. R., Nandy, S. K. and Gupta, A. S. (2012), "Oblique stagnation-point flow and heat transfer towards a shrinking sheet with thermal radiation", *Mechanical*, 47(6): 1325–1335, doi:10.1007/s11012-011-9516-z.

Makinde, O. D. and Aziz, A. 2011, "Boundary layer flow of a nanofluid past a stretching sheet with a convective boundary condition", *International Journal of Thermal Sciences*, 50(7): 1326-1332,

doi: https://doi.org/10.1016/j.ijthermalsci.2011.02.019.

Makinde, O. D., Khan, W. A. and Khan, Z. H.2016, "Non-aligned MHD stagnation point flow of variable viscosity nanofluids past a stretching sheet with radiative heat", *Journal of Heat and Mass Transfer*, 96: 525-534,
doi:10.1016/j.ijheatmasstransfer.2016.01.052

Megahed, A. M. and Abbas, W. 2022, "Non-Newtonian Cross fluid flow through a porous medium with regard to the effect of chemical reaction and thermal stratification phenomenon", *Case Studies in Thermal Engineering*, 29:101715,
doi: https://doi.org/10.1016/j.csite.2021.101715.

Mehmood, R., Nadeem, S. and Akbar, N. S. 2015, "Partial slip effect on non-aligned stagnation point nanofluid over a stretching convective surface", *Chinese Physics B*, 24(1):014702, doi: 10.1088/1674-1056/24/1/014702.

Nadeem, S., Mehmood, R. and Akbar, N. S.2013, "Non-orthogonal stagnation point flow of a nano non-Newtonian fluid towards a stretching surface with heat transfer", *International Journal of Heat and Mass Transfer*, Vol.57 No.2, pp.679–689,
doi: https://doi.org/10.1016/j.ijheatmasstransfer.2012.10.019.

Rajendar, P., AnandBabu, L. and VijayaLaxmi, T. 2017, "MHD Stagnation Point Flow and Heat Transfer Due to Nano Fluid over Exponential Radiating Stretching Sheet", *Global Journal of Pure and Applied Mathematics*, 13(6):1593-1610.

Raptis, A. A. and Takhar, H. S. 1987, "Flow through a porous medium", *Mechanics Research Communications*, 14(5):327–329,
doi: https://doi.org/10.1016/0093-6413(87)90049-8.

Reddy, N. N., Rao, V. S. and Reddy, B. R. 2021, "Chemical reaction impact on MHD natural convection flow through porous medium past an exponentially stretching sheet in presence of heat source/sink and viscous dissipation", *Case Studies in Thermal Engine*, 25:100879. doi:https://doi.org/10.1016/j.csite.2021.100879.

Rehman, A., Nadeem, S. and Malik, M. Y. 2013, "Stagnation flow of couple stress nanofluid over an exponentially stretching sheet through a porous medium", *Journal of Power Technologies*, 93(2):122–132.

Reza, M. and Gupta, A.S. 2005, "Steady two-dimensional oblique stagnation-point flow towards a stretching surface", *Fluid Dynamics Research*, 37(5):334–340,
doi: 10.1016/j.fluiddyn.2005.07.001.

Rizwan, UlH.andNadeem, S.2014, "Effect of Thermal Radiation for Megneto-hydrodynamic Boundary Layer Flow of a Nanofluid Past a Stretching Sheet with Convective Boundary Conditions", *Journal of Computational and Theoretical Nanoscience*, 11(1):32–40, doi: https://doi.org/10.1166/jctn.2014.3313.

Seddeek, M. A.2007, "Heat and mass transfer on a stretching sheet with a magnetic field in a visco-elastic fluid flow through a porous medium with heat source or sink", *Computational Materials Science*, 38(4):781–787,
doi: https://doi.org/10.1016/j.commatsci.2006.05.015.

Sepasgozar, S., Faraji, M. and Valipour, P.2017, "Application of differential transformation method (DTM) for heat and mass transfer in a porous channel",*Propulsion and Power Research*, 6(1):41-48,
doi:https://doi.org/10.1016/j.jppr.2017.01.001.

Stuart, J.T. 1959,"The viscous flow near a stagnation point when external flow has uniform vorticity", *Journal of the Aerospace Sciences*, 26(2):124–125,
doi:https://doi.org/10.2514/8.7963.

Tamada, Ko.1979, "Two-dimensional stagnation-point flow impinging obliquely on a plane wall", *Journal of the Physical Society of Japan*, 46(1):310–311,
doi: https://doi.org/10.1143/JPSJ.46.310.

Uka, U. A. and Amos, E. 2022, "Hydromagnetic Nanofluid Flow over an Exponentially Stretching Sheet in the Presence of Radiation and Nonuniform Heat Generation/Absorption", *IOSR Journal of Mathematics*, 18(1): 31-43,
doi: 10.9790/5728-1801023143.

Ullah, I., Jafar, A. B. and Shafie, S. 2020, "MHD radiative nanofluid flow induced by a nonlinear stretching sheet in a porous medium", *Heliyon*, 6(6): e04201,
doi: 10.1016/j.heliyon.2020.e04201.

Vijaya, N., VenkataRamana Reddy, G. and Hara Krishna, Y.2019, "Non-Aligned Stagnation Point Flow of a Casson Fluid Past a Stretching Sheet in a Doubly Stratified Medium", *Fluid Dynamics & Materials Processing*, 15(3):.233-251, doi: 10.32604/fdmp.2019.03727.